SLAC-PUB-13248
May 2008

STREAK-CAMERA MEASUREMENTS WITH HIGH CURRENTS IN PEP-II AND VARIABLE OPTICS IN SPEAR3*

Weixing Cheng,# Alan Fisher, and Jeff Corbett
Stanford Linear Accelerator Center, 2575 Sand Hill Road, Menlo Park, CA 94025

Abstract

A dual-axis, synchroscan streak camera was used to measure longitudinal bunch profiles in three storage rings at SLAC: the PEP-II low- and high-energy rings, and SPEAR3. At high currents, both PEP rings exhibit a transient synchronous-phase shift along the bunch train due to RF-cavity beam loading. Bunch length and profile asymmetry were measured along the train for a range of beam currents. To avoid the noise inherent in a dual-axis sweep, we accumulated single-axis synchroscan images while applying a 50-ns gate to the microchannel plate. To improve the extinction ratio, an upstream mirror pivoting at 1 kHz was synchronized with the 2kHz MCP gate to deflect light from other bunches off the photocathode. Bunch length was also measured on the HER as a function of beam energy. For SPEAR3 we measured bunch length as a function of single-bunch current for several lattices: achromatic, low-emittance and low momentum compaction. In the first two cases, resistive and reactive impedance components can be extracted from the longitudinal bunch profiles. In the low-alpha configurations, we observed natural bunch lengths approaching the camera resolution, requiring special care to remove instrumental effects, and saw evidence of periodic bursting.

INTRODUCTION

The Stanford Linear Accelerator Center (SLAC) has a long history of both high-energy physics (HEP) and synchrotron radiation (SR) research with storage rings. Recently, PEP-II and SPEAR3 (Table 1) together purchased a Hamamatsu C5680 streak camera with ~2-ps resolution, digital image capture, and dual-axis synchroscan sweeping to measure bunch length, characterize impedance, and observe beam instabilities.

PEP-II

The PEP-II *B* Factory completed its final run on April 7, 2008. Since the first beam in 1997, the PEP rings have run at a center-of-mass energy of 10.58 GeV, the Y(4S) resonance. Electrons at 8.97 GeV in the high-energy ring (HER) collide with 3.12-GeV positrons in the low-energy ring (LER) to produce $B\bar{B}$ pairs moving in the lab frame. For the final months of the 2008 run, the HER energy was shifted to collide at the 2S (10.02 GeV) and 3S (10.36), and then scanned up from just below the 4S to 11.2 GeV. This provided an opportunity to measure bunch length over a range of HER energies from 8.02 to 10.08 GeV.

Each PEP-II ring has a synchrotron-light monitor (SLM) observing visible dipole radiation [1]. The LER SLM collects positron emission from a dipole 30 m downstream of the interaction point (IP), while the HER SLM collects electron emission from an arc dipole. At each SLM, in-tunnel CCD cameras record beam images and interferometer fringes [2], and a visible-light transport line brings part of the beam to a focused image in an optics hutch outside the shielding wall for more sophisticated time-resolved cameras [3,4].

In the last year of PEP-II operations, the new streak camera was first installed in the LER hutch to resolve bunch-length discrepancies observed in 2004 when comparing a quick series of measurements with a borrowed streak camera to the high-frequency roll-off of the bunch spectrum [3]. The camera was then moved to the HER to track bunch length during the energy scan.

Since the beams collide at high current—typically 1.75 A in the HER and 2.6 A in the LER, for a peak luminosity of 1.0×10^{34} $cm^{-2}s^{-1}$—the gradual increase in beam loading following the 100-ns abort gap in the fill pattern causes a shift in synchronous phase, so that bunches further along the train arrive earlier in the RF period. At high-currents, the transient from first to last bunch is comparable to the natural rms bunch length (~40 ps in the LER). To measure bunch length without folding in the phase shift of the entire train required dual approaches to select a narrow interval: an electronic gate of the camera's microchannel plate (MCP), and an oscillating mirror that synchronously steers the light across the entrance optics.

SPEAR3

SPEAR3 is a 3-GeV storage-ring light source delivering UV to x-ray radiation into 13 beam lines (~30 branch lines) in a 500 mA, multi-bunch mode. The machine lattice was recently adjusted from achromatic (zero-dispersion) to finite-dispersion optics to reduce horizontal emittance, and tests have begun on low-momentum-compaction (low-α) lattices for dynamical pump-probe experiments. The SLM at SPEAR3 receives unfocused

Table 1: Key PEP-II and SPEAR3 parameters.

	PEP-II		SPEAR3
	HER	LER	
Energy (GeV)	9 (8–10)*	3.12	3
f_{RF} (MHz)	476	476	476.315
Harmonic No.	3492	3492	372
Bunches**	1722	1722	280
Spacing (ns)	4.2	4.2	2.1

* Energy varies during the CM-energy scan.

** Typical multi-bunch fill. PEP-II fills every 2nd bucket outside a 100-ns abort gap. SPEAR3 fills every bucket, with a single bunch in a 100-ns ion clearing gap.

* Work sponsored by U.S. Department of Energy Contract DE-AC02-76SF00515 and Office of Basic Energy Sciences, Division of Chemical Sciences.

chengwx@slac.stanford.edu

visible light through a 420-nm long-pass filter and a 6-in-diameter lens with a 2-m focal length. The light is relayed to several diagnostic instruments, including the streak camera [5,6]. The nominal bunch length is ~20 ps rms but can be as short as ~2 ps in the low-α mode, a value comparable to the C5680 streak-camera resolution.

STREAK-CAMERA OPERATION

Single- and Dual-Axis Synchroscan

The most basic operation of a streak camera uses a triggered sweep to measure the longitudinal intensity profile of a light pulse. Visible SR from the single passage of a bunch, however, is generally weak, producing an image dominated by shot noise that severely increases the χ^2 of a Gaussian fit. On the other hand, if more intensity is available, space charge at the photocathode can broaden the profile, again leading to erroneous results. Superposition of repeated low-light measurements is compromised by random trigger jitter. The dual-sweep mode (fast [ps] vertical, slow [100 ns to 100 ms] horizontal) is still subject to both shot noise and jitter in the fast-axis trigger.

An alternative is "synchroscan" mode, in which a large-amplitude sinusoid at a sub-harmonic of the storage ring's master oscillator drives the streak-camera sweep. Photoelectrons are dispersed across the MCP only during the linear part of the sine, near the zero crossings. Repeated low-light images are summed over a long exposure (typically 120 ms) on the camera's CCD to produce an image with little space-charge broadening, shot noise, or jitter.

At high currents in PEP-II, the slew in synchronous phase along the bunch pattern is comparable to the bunch length. Single-axis synchroscan overlaps bunches with centroids at different arrival times, broadening the measured length. In dual-axis synchroscan mode, the camera separates the image of each SR pulse in the bunch train, highlighting this slew. The instantaneous profile can be found by combining nearby bunches in software, but the Gaussian fits still suffer from noise. Instead, we combine single-sweep synchroscan with electronic and mechanical gating to repeatedly transmit light from only a few bunches along the train over a long exposure.

In SPEAR3, beam loading is not severe, but ~1-ps RF phase jitter eventually masks the true bunch-length measurements in the short-pulse mode as α is reduced. Attempts have been made to remove phase noise by fitting a series of pulse-by-pulse measurements in the dual-scan mode, but again shot-noise makes this method less satisfactory than synchroscan. Also, the low-α studies have seen a "bursting" phenomenon (discussed below), perhaps from a semi-periodic relaxation oscillation leading to emittance blow-up, which may be best explored using electronic/mechanical gating.

Electronic Gating

The PEP-II bunch length can be measured despite the synchronous-phase slew along the train by combining (single-axis) synchroscan with a narrow MCP gate locked to the ring clock, in order to superpose images from many turns, but from the same slice within the bunch train.

The MCP gate on the Hamamatsu C5680 has a minimum width τ_g = 50 ns and a maximum repetition rate f_g = 10 kHz. For accurate measurements, the MCP gate must provide sufficient extinction to block unwanted light from the remaining bunches. A 7.3-μs PEP-II turn contains 1722 bunches spaced by 4.2 ns ($2/f_{RF}$). Neglecting the 100-ns (1.4%) beam-abort gap, the necessary extinction ratio is $\tau_g f_g = 5\times10^{-4}$, easily within the factory specification of 10^{-6}. Since the PEP-II synchroscan drive is at $f_{RF}/4$ (119 MHz, half the bunch rate), a small phase shift from the zero crossing separates the even and odd bunches into two images located above and below the screen's center. Each spot combines bunches separated in time by 8.4 ns, putting 6 bunches in the 50-ns MCP gate.

Adding the MCP gate clearly reduces the image brightness. It drops further when the gate timing is centered on the abort gap, but does not completely darken. Instead the gap image shows a background spot slightly shifted from the bunch-train image and of comparable intensity (Fig. 1(a)). Further evidence of poor extinction is a variation seen in bunch length along the train, especially at the head where the synchronous phase changes most rapidly. While discussing this leakage with Hamamatsu, we pursued alternative ways to extract the true bunch length.

Scanning Mirror

In PEP-II, visible light is relayed to the streak camera through a 450-nm filter with a full width of 30 nm, and focused onto the entrance slit by a microscope objective. To improve the extinction ratio, we installed a scanning galvanometer (GSI Lumonics VM500S)—a small, flat mirror mounted on the shaft of a DC motor—upstream of the objective. Such devices are found in laser scanners for light shows, displays, and printers, and are often used in pairs for raster scans. Since they turn rapidly, one was used in a previous experiment that scanned light across the photocathode of a gated camera to observe the turn-to-turn evolution of transverse beam sizes in PEP-II during the onset of beam instability and during injection [4].

A driver board (also GSI Lumonics) pivots the mirror at an angle proportional to a control voltage. As a sinusoidal drive turns the mirror through ±2°, the incident SR light sweeps horizontally well beyond the acceptance of the objective, passing through it at each zero crossing of the angle. Sweeping the beam orthogonally to the (vertical) fast time axis avoids blurring the time resolution. Since mirror inertia limits the sinusoidal drive to 1 kHz, we slow the MCP

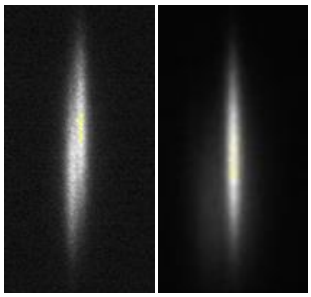

(a) (b)

Figure 1: (a) Streak image with synchroscan and 50-ns MCP gate. The image to the lower left is leakage through the gate. (b) Image with MCP gate plus rotating mirror, for minimal leakage.

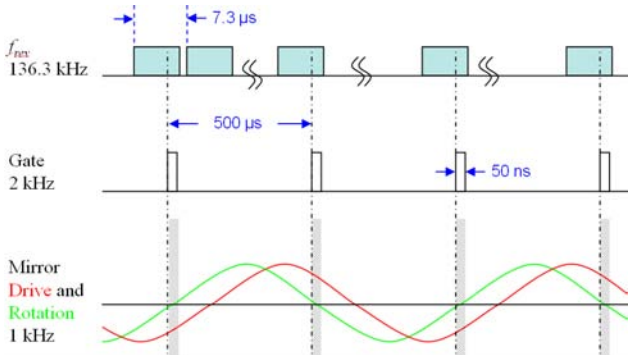

Figure 2: Timing of bunch pattern (top), streak-camera gate (middle) and rotating mirror (bottom).

gate to 2 kHz (every zero crossing, Fig. 2).

To synchronize the MCP gate with the mirror's zero crossings, the 136-kHz ring-turn (f_{rev}) clock triggers a digital delay generator (SRS DG535) with four delays. One, set to 499 μs, slows the retrigger rate to ~2 kHz, locked to the next ring turn. Two delays start and stop the 50-ns MCP gate. The fourth triggers a function generator (SRS DS345) set to produce a single-period, 1-kHz sine wave, starting at −270° to provide a delay before its zero crossing. The DS345 waits for its 1-ms output to finish before retriggering. The result is a continuous 1-kHz sine wave rotating the mirror through ±2° at a phase locked to the ring-turn clock and to the MCP gate.

To align the mirror, we first set the drive amplitude to zero, using a DC offset from the DS345 to aim the light through the middle of the objective lens onto the center of the streak camera photocathode. Next the drive was slowly increased while an oscilloscope displayed both the drive and readback signals for the mirror angle. This allowed us to determine the maximum drive amplitude at 1 kHz (400 mV peak) and to measure the inertial lag of the mirror zero crossing (Fig. 2) relative to its trigger.

These settings were sufficient to see MCP-gated light on the streak camera at both of the mirror zero crossings. Small delays (tens of ns) of the gate then merged the two zero-crossing images. With this combined electronic and mechanical gating, the residual leakage in the abort gap was reduced to only a weak horizontal smear apertured on either side by the size of the objective lens. Most of this background was excluded from our analysis by software selecting a narrow region of interest for profiling; any remainder was measured and subtracted.

ANALYSIS OF BUNCH-PROFILE IMAGES

The impedance of a storage ring both stretches and skews the Gaussian form of the longitudinal bunch profile as the single-bunch current increases. Wakefields generated at the head of the bunch couple to the tail via resistive and reactive broadband impedance elements. The former elements steepen the head of the bunch compared to the tail, while the latter mainly increase bunch length (potential-well distortion) [7]. In general, the combination of wakefield impedance and energy spread distorts the longitudinal bunch distribution away from an ideal Gaussian as single-bunch current increases.

Consequently, we used an asymmetric Gaussian profile:

$$I(z) = I_0 + I_1 \exp\left\{-\frac{1}{2}\left(\frac{(z-z_0)}{[1+\mathrm{sgn}(z-z_0)A]\sigma}\right)^2\right\} \quad (1)$$

where A is a scalar asymmetry factor and z_0 locates the distribution offset, to fit projections of a user-specified region of interest in the synchroscan image. At low bunch currents, there is no asymmetry, and so we set A to 0 to reduce numerical noise.

Below the microwave threshold, we can fit the measured bunch lengthening versus bunch current I_b to Zotter's potential-well distortion formula [7]:

$$\left(\frac{\sigma_z}{\sigma_{z0}}\right)^3 - \frac{\sigma_z}{\sigma_{z0}} = \frac{1}{\sqrt{2\pi}} \frac{\alpha_c e I_b}{E_0 \nu_{s0}^2} \left(\frac{c}{\omega_{\mathrm{rev}} \sigma_{z0}}\right)^3 \mathrm{Im}\left[\left(\frac{Z}{n}\right)_{\mathrm{eff}}\right] \quad (2)$$

to find the reactive component of the effective impedance and so estimate the ring's broadband inductance L:

$$L\omega_{\mathrm{rev}} = \mathrm{Im}\left[(Z/n)_{\mathrm{eff}}\right] \quad (3)$$

Here E_0 is the beam energy and ν_{s0} is the low-current synchrotron tune.

Above the current threshold for the longitudinal microwave instability, energy spread further increases bunch length, according to Chao-Gareyte scaling [8]; then an asymmetric Gaussian provides an adequate but less accurate fit. This was a consideration only for SPEAR3 since PEP-II bunch currents are below this threshold.

MEASUREMENTS ON PEP-II

Data was taken under three conditions: in a full ring, during filling, and—for the LER—with a single test bunch filled in small increments. The first two cases involved parasitic measurements during routine collisions, and required both gates. The single-bunch data (which needed no gating) was obtained in a dedicated experiment in the final hours of the 2008 run.

PEP's bunch-current monitor (BCM) measures the charge in each ring's 3492 buckets at 1 Hz [1]. The bunch-injection controller (BIC) computer then arranges injection to fill each ring in a user-specified pattern (normally a uniform fill). After filling, the charge in each bunch is kept steady with small injections at a few Hz as needed ("trickle charge"). Thus streak-camera images taken with the ring current at its goal have a well-determined bunch charge within the MCP gate. During fills, the charge in the gate is less certain, as the linac timing shifts to fill different bunches, and histories of the BCM readings and filling sequence are not recorded.

Figure 3 shows measurements with 2150 mA in the LER, using a 50-ns MCP gate plus the rotating mirror, both delayed in 100-ns steps. Unlike measurements with only the MCP gate, here we see a constant the bunch length (36.9 ps) and Gaussian asymmetry factor (-0.06).

The synchronous phase clearly changes due to beam loading. Unfortunately, the RF phase at the LER optics hutch, at the end of the RF transport line, is poorly stabilized, drifting by 10 to 20 ps over hours and sometimes minutes. Consequently, the streak image moves on

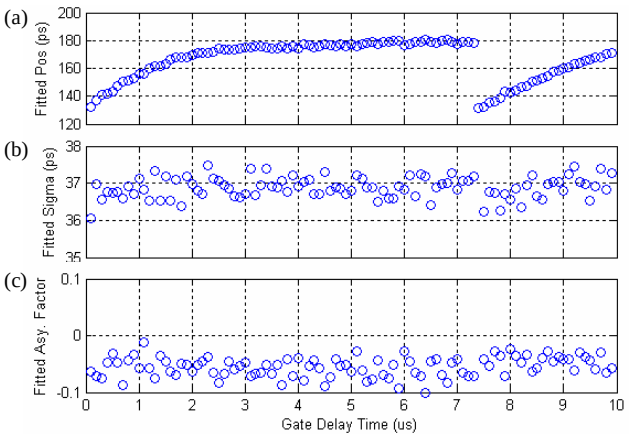

Figure 3: Measurements along a train of 1722 LER bunches, using a 50-ns gate delayed in 100-ns increments from the abort gap. (a) Location of fitted peak z_0, which slews by ~50 ps, corresponding to $\Delta\phi_s = 8.6°$ of RF. The gap returns after 1 turn, 7.3 μs. (b) Bunch length (rms) σ. (c) Asymmetry factor A.

the screen, complicating relative phase measurements for scans in collision. However, the experiment varying the charge in a single test bunch from 0 to 3 mA (Fig. 4) included a comparable total charge in several low-charge reference bunches, placed 180° of the 119-MHz drive away from the test bunch. The images of the reference bunches then overlapped on the streak camera at a different location from the test-bunch image, allowing a measure of the phase slew independent of the RF drift.

In the HER, we measured the bunch length versus bunch current (Fig. 5) and energy (Fig. 6). The RF voltage was reduced from 16.5 to 14 MV for the low-energy point at the Y(2S) resonance. As with the LER, the phase transient along the bunch train due to beam loading required both the MCP gate and rotating mirror. The HER's bunch lengthening is smaller than the LER's due to a lower chamber impedance, and the asymmetry is negligible.

MEASUREMENTS ON SPEAR3

SPEAR3 recently retuned the original achromatic (AC) optics by adding finite dispersion in the ID straight sections. The corresponding change in lattice partition numbers gives the new low-emittance (LE) optics an

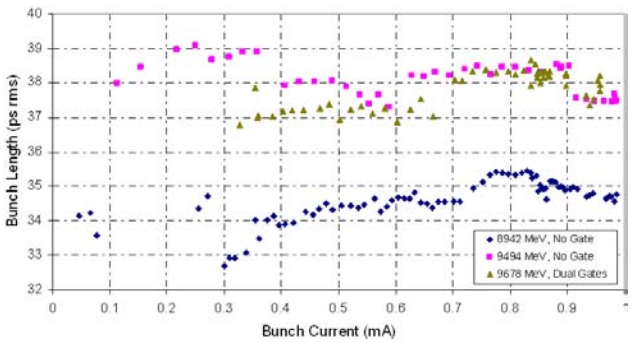

Figure 5: HER bunch length vs. bunch current at three energies. Using dual gates at 9.7 MeV reduced the measured length compared to 9.5 MeV without gating.

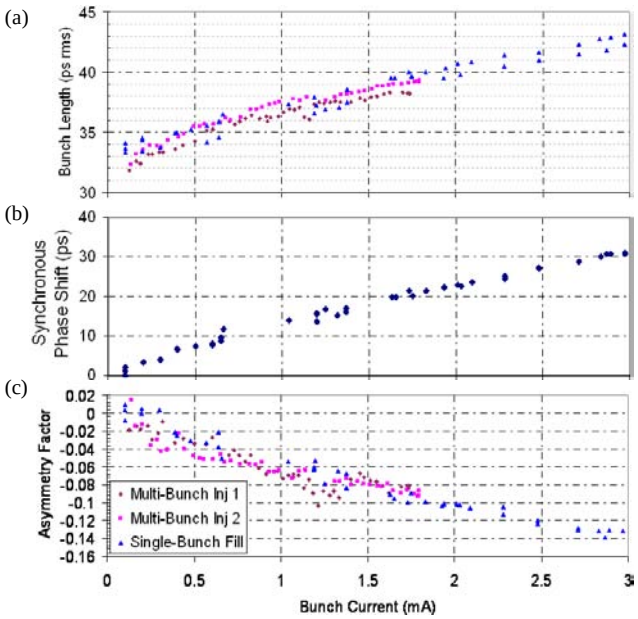

Figure 4: LER data vs. bunch current. (a) Bunch length σ. (b) Synchronous-phase shift $\Delta\phi_s$. (c) Asymmetry factor A.

emittance just below 10 nm·rad, rather than 16, but increases the natural bunch length from 17 to 20.4 ps. As the ring moves toward top-off operation at 500 mA and adds more IDs, it is important to understand bunch lengthening, beam lifetime, and associated impedance effects with the LE optics. The low-α (LA) lattices are equally important, but in many ways more challenging [9], in part because the short bunches approach the resolution limit of the C5680 streak camera. Special care is therefore needed to verify the expected $\alpha^{½}$ scaling.

Bunch-length measurements were made for all three optical configurations as a function of single bunch current (Fig. 7) in single-axis synchroscan mode. For the AC and LE optics, the natural bunch length agrees with theory but can vary by 1 to 2 ps between measurements taken several weeks apart. Both lattices show a "knee" in the bunch-length curves near 7 mA, which may be the onset of the microwave instability; we are actively pursuing this effect. Fitting the low-current data to asymmetric Gaussian profiles and using Zotter's formula for potential-well distortion yields $|Z/n| \approx 0.28\ \Omega$ or L ≈35 nH.

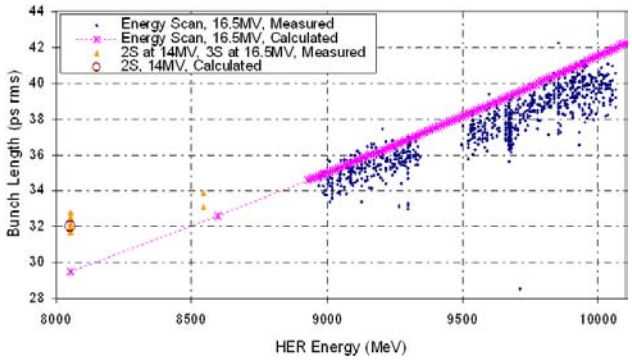

Figure 6: HER bunch length vs. energy for ring currents between 1500 and 1750 mA. V_{RF} = 14 MV for Y(2S) at 8 GeV, 16.5 MV for all others.

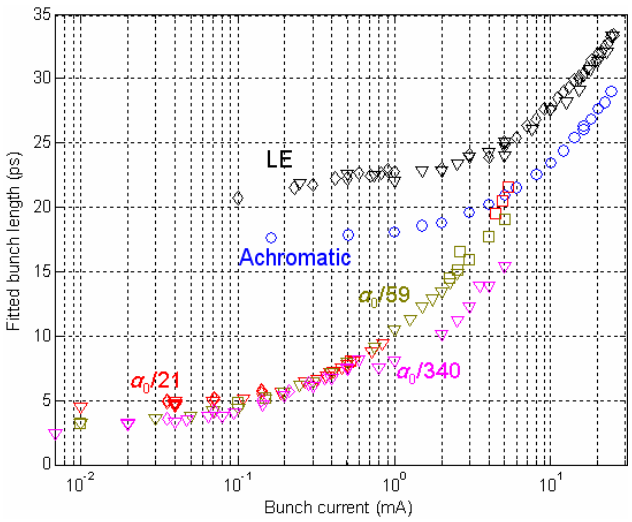

Figure 7: Bunch length (rms) versus single-bunch current in SPEAR3 for different lattices.

The low-α case is more complicated because rapid bunch lengthening begins at very low current. Decreasing α by a factor of 60 lowers the natural bunch length below 2.5 ps rms, which is suitable for some short-pulse SR research, albeit at low single-bunch currents. The injected current must be kept below 10 μA to preserve the natural bunch length, yielding low light levels to experimentalists and on the photocathode.

Before correcting for streak-camera resolution, Fig. 7 shows low-current bunch lengths of 4.5, 3.2 and 2.5 ps rms for α_0/21, α_0/59 and α_0/340 respectively, whereas direct $\alpha^{½}$ scaling from the AC optics predicts lengths of 3.7, 2.2, and 0.9 ps rms. The common correction subtracts in quadrature the minimum spot size measured with the streak camera in "focus mode" (no streak deflection). We measured this value to be 5.0 pixels FWHM, which converts to 0.32 ps rms (0.75 ps FWHM) in the most sensitive range (R1), below the camera's specified resolution of 2 ps FWHM. However, other broadening effects apply, including dispersion of the photoelectrons emitted at the cathode and a lower space charge in focus mode. The 2-ps specification is also based on single-shot measurements with a short 800-nm laser pulse; dispersion is greater at our 550-nm wavelength. Synchroscan introduces additional broadening effects: jitter on the beam's RF (~1 ps rms) and the synchroscan drive, and dipole-mode synchrotron oscillations of the beam. As a result, an effective R1 resolution of ~2.4 ps rms (5.6 ps FWHM) is needed to make all three measurements consistent with predictions.

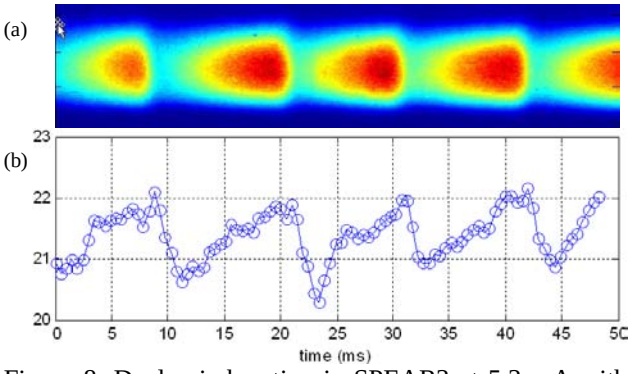

Figure 8: Dual-axis bursting in SPEAR3 at 5.3 mA with the α_0/21 lattice. (a) Dual-axis streak image. (b) Bunch length (ps rms) from this image.

Finally, with LA optics the total injected charge is limited to ~1 mA/bunch unless the RF voltage is reduced below 2 MV from 3.2 MV. Above ~3mA/bunch, the α_0/21 lattice exhibits quasi-periodic bursts in synchrotron-radiation intensity and increased bunch length (Fig. 8) [10].

SUMMARY

Streak-camera measurements of bunch length and profile asymmetry at high currents in the PEP-II rings require a novel electronic/mechanical gating configuration to remove the effect of slew in synchronous phase following the abort gap. Bunch-length measurements in SPEAR3 yield an inductive impedance of $|Z/n| \approx 0.28\ \Omega$ and with low-α lattices require careful evaluation of the camera's true resolution limit in synchroscan mode.

ACKNOWLEDGEMENTS

We gratefully acknowledge the advice and assistance of Alex Lumpkin, Walter Mok, Jim Sebek and Bill Cieslik.

REFERENCES

[1] A.S. Fisher, "Instrumentation and Diagnostics for PEP-II," BIW98, Stanford, CA, 4–7 May 1998, p. 95.
[2] A.S. Fisher, E.L. Bong, R.L. Holtzapple, and M. Petree, "Beam-Size Measurements on PEP-II Using Synchrotron-Light Interferometry," PAC01, Chicago, IL, 18–22 June 2001, p. 547.
[3] A.S. Fisher *et al.*, "Bunch-Length Measurements in PEP-II," PAC05, Knoxville, TN, 16–20 May 2005, p. 1934.
[4] A.S. Fisher *et al.*, "Turn-by-Turn Imaging of the Transverse Beam Profile in PEP-II," BIW06, Batavia, IL, 1–4 May 2006, p. 303.
[5] W.J. Corbett, C. Limborg-Deprey, A.Y. Mok and A. Ringwall, "The SPEAR3 Diagnostic Beam Line," PAC05, Knoxville, TN, 16–20 May 2005, p. 4057.
[6] W.J. Corbett *et al.*, "Bunch-Length Measurements in SPEAR3," PAC07, Albuquerque, NM, 25–29 June 2007, p. 4159.
[7] B. Zotter, "Potential-Well Bunch Lengthening," CERN SPS/81-14 (1981).
[8] A.W. Chao and J. Gareyte, "Scaling Law for Bunch Lengthening in SPEAR-II," Part. Accel. **25** (1990) 229.
[9] X. Huang *et al.*, "Low-Alpha Mode for SPEAR3," PAC 2007, Albuquerque, NM, 25–29 June07, p. 1308.
[10] W. Cheng *et al.*, "Bunch Length and Impedance Measurements at SPEAR3," EPAC08, Genoa, Italy, 23–27 June 2008.